Reprint Series
25 May 1984, Volume 224, pp. 869–872

SCIENCE

Seismic Potential Revealed by Surface Folding: 1983 Coalinga, California, Earthquake

Ross S. Stein and Geoffrey C. P. King

References and Notes

1. L. W. Alvarez, W. Alvarez, F. Asaro, H. V. Michel, *Science* **208**, 1095 (1980).
2. W. Alvarez *et al.*, *Geol. Soc. Am. Spec. Pap. 190* (1982), pp. 305–315.
3. C. J. Orth *et al.*, *Science* **214**, 1341 (1981).
4. M. R. Rampino [*Geol. Soc. Am. Spec. Pap. 190* (1982), pp. 423–433] makes a case for concentration of iridium in marine clays at the K-T boundary by solution of pelagic limestones. This scenario cannot be applied to nonmarine boundary clays located in siliclastic rocks.
5. Altered volcanic tuffs in coal beds (tonsteins) have been extensively studied (by B.F.B. and D.M.T.) throughout the United States. Techniques for determining the original volcanic derivation of these claystones by whole sample analysis can be found in D. M. Triplehorn and B. F. Bohor [*U.S. Geol. Surv. Open-File Rept. 81-775* (1981)]; and B. F. Bohor and D. M. Triplehorn [*Guideb. Geol. Soc. Am. Annu. Coal Div. Field Trip* (1981), pp. 49–54].
6. The boundary claystone was found in the vicinity of a stratigraphic section near Brownie Butte described by R. H. Tschudy [*Geol. Soc. Am. Spec. Pap. 127* (1970), pp. 65–111].
7. Single-point instrumental neutron activation analysis of the claystone layer by C. J. Orth at Los Alamos Scientific Laboratories. Similar analyses by Orth of samples 30 cm above and below the boundary layer gave background values for iridium of 5.0 and 8.0 parts per trillion, respectively.
8. Palynologic analyses by R. H. Tschudy, U.S. Geological Survey, Denver, Colo.
9. B. F. Bohor, paper presented at the 20th Annual Meeting of the Clay Minerals Society, Buffalo, N.Y., October 1983.
10. C. B. Sclar, N. M. Short, G. G. Cocks, in *Shock Metamorphism of Natural Materials*, B. M. French and N. M. Short, Eds. (Mono Book, Baltimore, 1968), pp. 483–493.
11. W. v. Englehart and D. Stöffler, in *ibid.* pp. 159–168.
12. E. T. C. Chao, in *ibid.* pp. 135–158.
13. N. L. Carter, *Am. J. Sci.* **263**, 786 (1965).
14. D. Stöffler, *Fortschr. Mineral.* **49**, 50 (1972).
15. W. v. Englehart and W. Bertsch, *Contrib. Mineral. Petrol.* **20**, 203 (1969).
16. N. M. Short, in *Shock Metamorphism of Natural Materials*, B. M. French and N. M. Short, Eds. (Mono Book, Baltimore, 1968), pp. 185–210; F. Horz, in *ibid.* pp. 243–253.
17. T. E. Bunch, in *ibid.* pp. 413–432.
18. F. Dachille, P. Gigl, P. Y. Simons, in *ibid.* pp. 555–569; F. Horz and W. L. Quaide, *Lunar Planet. Sci. Inst. Contrib. 02* (1970).

19. We thank C. J. Orth and R. H. Tschudy for their analyses; E. Shoemaker, B. French, D. Stöffler, and A. Gratz for their helpful comments; and C. Sanderson for laboratory assistance.

24 January 1984; accepted 16 February 1984

Seismic Potential Revealed by Surface Folding: 1983 Coalinga, California, Earthquake

Abstract. *The 2 May 1983 Coalinga, California, earthquake (magnitude 6.5) failed to rupture through surface deposits and, instead, elastically folded the top few kilometers of the crust. The subsurface rate of fault slip and the earthquake repeat time are estimated from seismic, geodetic, and geologic data. Three larger earthquakes (up to magnitude 7.5) during the past 20 years are also shown to have struck on reverse faults concealed beneath active folds.*

Identification of past and future earthquake sources is a fundamental goal of earthquake-hazard reduction. The principal strategy is to locate active faults, determine their most recent slip event, and estimate their slip rate and earthquake repeat time. Most active faults are manifested at the earth's surface by displaced young deposits or by fault scarps. Faults that do not reach the surface or do not cut surface deposits are not recognized or are classed as inactive unless they can be independently identified by strain accumulation at the surface or by seismicity at depth.

The 1983 Coalinga, California, earthquake of magnitude (M_s) 6.5 provides a striking illustration of slip on an active but concealed fault that had not been detected by seismic reflection and network microseismicity. We present evidence that the fault slipped about 2 m over a depth of 4 to 12 km, unaccompanied by surface rupture except during one aftershock (*1*, *2*). Despite an estimated 2 km of cumulative fault slip during the past 1 to 2 million years, no major fault scarp has formed. We also consider three other larger and well-studied thrust earthquakes that were accompanied by surface folding and decreased surface rupture in comparison with the slip at depth and contend that, in some tectonic environments, folds form as a consequence of repeated subsurface thrust events. Because the peak ground motion associated with thrust earthquakes appears to be two to three times higher than that observed for normal slip events of the same size (*3*), active folds should be regarded as sites of critical earthquake risk.

Reverse faults that rupture to the earth's surface leave a scarp along the edge of the upthrown fault block; commonly, a prism of sediments accumulates on the downthrown block (Fig. 1, A and B). Whereas slip in great shallow earthquakes, such as the 1906 strike-slip shock on the San Andreas fault in California (*4*), tends to be nearly constant as a function of depth, moderate to large thrust earthquakes typically display less slip at the surface than at depth (*5*). Thrust events that do not extend to the surface deform the rocks above the fault into a gentle fold, do not create a fault scarp, and typically result in the deposition of only a thin veneer of superficial sediments (Fig. 1, C and D). Because most faults in the brittle-elastic layer of the crust cause displacement largely during earthquakes, overlying folds must be built by repeated shocks.

Faults can slip repeatedly without reaching the earth's surface if the stresses at the fault tip and those imposed on the overlying material can relax between earthquakes. Because these stresses can

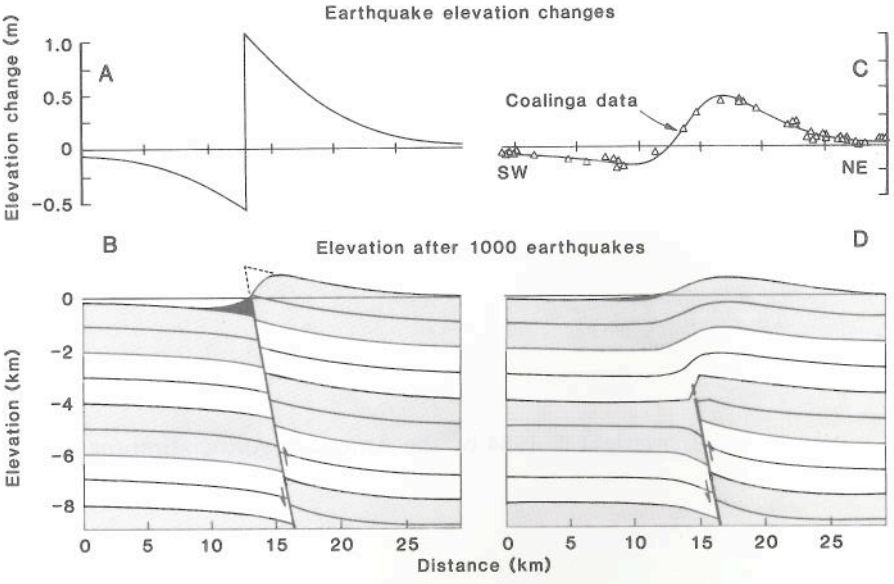

Fig. 1. (A) Elastic dislocation solution for surface deformation caused by 2 m of reverse dip slip on a fault dipping 65° and extending from the ground surface to a depth of 11 km. (B) Depth cross section (vertical exaggeration ×2) after 2 km of cumulative slip, or 1000 earthquakes. Subsequent to initiation of faulting, erosion of fault scarp (dashed) and deposition into downthrown block (black) occur. Remote displacements and interseismic strain release are neglected. (C) Fault shown in (A) terminated 4 km from the surface, except fitted to the observed coseismic elevation changes at Coalinga (*1*). (D) Depth cross section for (C). Dip of beds above the top of the fault increases with depth, and near the top of the fault beds are subject to vertical compression and extension.

apparently be relieved by creep, by distribution along secondary fractures, by near-surface splay faults, or by chemical weathering, the near-surface rocks may not reach or be maintained at their failure stress. Flexural or bedding-plane slip between folded lithic units, and bending-moment faults that accommodate compressional and extensional fiber strains within the units, have been observed at the ground surface extending discontinuously to depths of 4 km in thoroughly drilled anticlines in California (*6*). Slip on these rootless faults, which do not continue at depth, may relieve the stresses caused by deep-seated events on reverse faults. The diffuse distribution of aftershocks that typifies all the concealed thrust events that we discuss (*7–9*) may be attributable to displacement on these secondary structures. Within the upper surface of an anticlinal hinge, extensional fiber stress may substantially exceed the regional horizontal compressive stress. Subject to this local stress deviation, unconsolidated near-surface deposits with low cohesive strength may form tensile cracks or grabens atop folds, masking evidence for thrust faulting.

Geodetic, geologic, and seismic data that constrain the Coalinga fault geometry and 1983 seismic slip suggest a history of intermittent displacement. Reverse slip on a fault dipping steeply to the northeast beneath Anticline Ridge satisfies the fault plane solution, hypocentral location, and seismic moment of the 2 May 1983 Coalinga earthquake, and also the coseismic elevation changes, although more complex fault geometries involving faults dipping southwest cannot be excluded. Geodetic elevation changes were determined by postearthquake measurement of bench marks previously surveyed in 1972. These geodetic data, corrected for ground subsidence caused by fluid pumping and for leveling-rod and atmospheric-refraction errors (*1*), are shown in Fig. 1C. The focal depth of the main shock is 10 to 12 km, with nodal planes striking northwest and dipping steeply northeast and gently southwest (*9, 10*). Because the aftershocks do not delineate a fault plane but, instead, cluster at depths of 5 to 12 km, we tested both fault orientations. The earthquake was modeled by uniform slip on a rectangular plane, with dislocations embedded in an elastic half-space. A steeply northeast dipping fault plane passing through the main shock (Fig. 2A) fits the data well (Fig. 1C), whereas a single fault dipping gently southwest at the depth of the main shock cannot satisfy the leveling data. The fault orientation was set equal to the seismic nodal plane, N53°W, 67°NE (*9*), and the wavelength of the coseismic surface deformation was used to estimate the depth to the top of the fault: 4 ± 1 km; the amplitude of this deformation was then used to determine the slip: 1.8 ± 0.5 m (*1*). Seismic reflection from the southern end of the aftershock zone reveals gently folded beds to a depth of about 4 km; beneath this depth, reflectors are sparse and discontinuous (*11*).

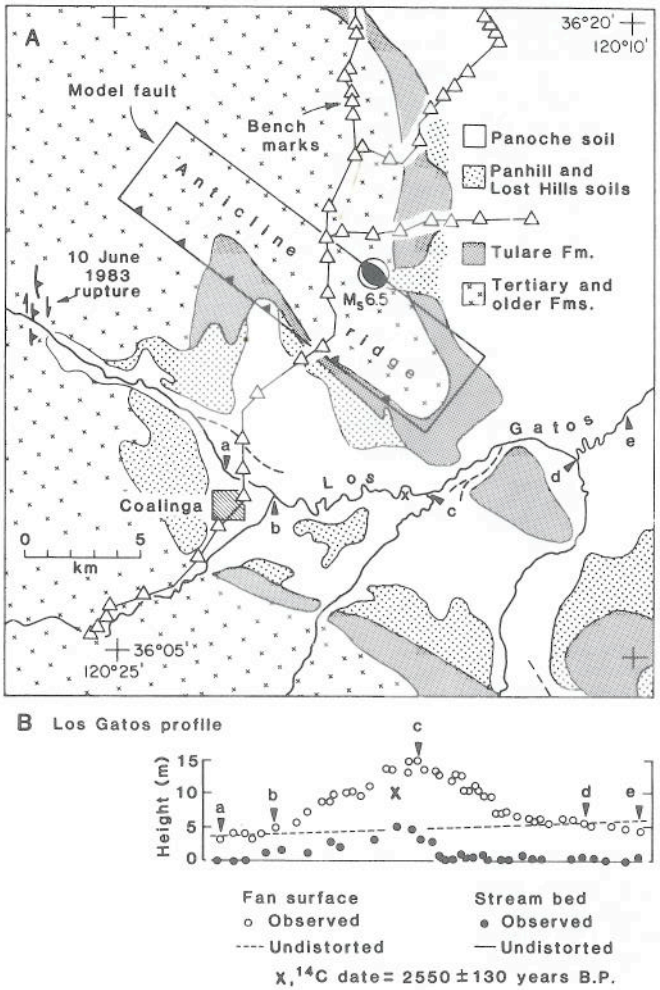

Fig. 2. (A) Soil (*14*) and geologic (*16*) units in the Coalinga area, showing surface projection of concealed fault plane (*1*), lower hemisphere projection of fault plane solution of the 2 May 1983 main shock (*9*), and the 10 June 1983 Nuñez fault rupture (*2*). Dashed lines indicate abandoned stream channels. (B) Profile of Los Gatos Creek where it passes through the anticline. An assumed equilibrium or undistorted stream bed gradient has been removed (*12*).

Los Gatos Creek cuts through the rising anticline near the site of the 1983 Coalinga earthquake and has left evidence of Holocene uplift (*12*). The creek meanders where its gradient has been increased by repeated subsidence events (site b, Fig. 2A), straightens as it passes through the anticline (site c), and meanders east of the uplift axis (site d). A profile of the stream bed and alluvial-fan surface was made from sites a to e (Fig. 2A) and a smooth convex-upward curve was fitted through the stream bed to represent its equilibrium profile (*13*). The residual from this curve is plotted in Fig. 2B. The stream has been unable to downcut as rapidly as the anticline has been uplifted, apparently deforming the bed profile. The stream bed and fan surface may also be elevated in this area because constriction of the stream channel where it passes through the anticline locally raises the hydraulic head. It is difficult to distinguish between the effects of topographic constriction and uplift of the anticline. Thus, uplift measured relative to the equilibrium profile should be considered a maximum value. The fan has been upwarped as much as 10 m in 2,500 to 10,000 years (*14*) at a position about 2 km southwest of the projected axis of peak coseismic uplift (Figs. 1C and 2A). This upwarp results in a maximum rate of surface uplift of 1 to 4 mm per year during the Holocene. When this rate is multiplied by the ratio of fault slip to surface uplift associated with the Coalinga earthquake (1.8 m/0.6 m), a subsurface fault-slip rate of 3 to 12 mm per year results. If the fault slips during earthquakes similar in size to the 1983 event, and no surface deformation occurs between earthquakes, then the slip rate yields a minimum repeat time of 200 to 600 years.

The profile of the 1983 Coalinga earthquake deformation (Fig. 1C) strikingly resembles the structure of Anticline

Ridge and the adjacent valley to the southwest and is similar to the simple elastic solution shown in Fig. 1D. Cumulative subsurface fault slip of at least 2 km during the past 2 million years, equivalent to 1000 events with slip similar to the 1983 earthquake, would explain this similarity (*15*). The youngest folded member is the Tulare Formation (Fig. 2A), 0.5 to 2.2 million years in age (*14, 16*). Because the base of the Tulare is nearly congruent with the underlying formations, the major episode of folding must postdate initial deposition of the Tulare Formation. This yields a slip rate of about 1 to 4 mm per year during the past 1 to 2 million years, and a repeat time of 500 to 1500 years if earthquakes are periodic and no shocks larger than the 1983 event have occurred. The estimates of average Pleistocene and maximum Holocene fault-slip rates at Coalinga overlap despite the use of different assumptions and methods, but the estimates also carry large uncertainties.

The 1980 El Asnam, Algeria, earthquake (M_s = 7.3) occurred within a major north African fold belt and beneath an anticlinal ridge (*17, 18*). The ridge was uplifted 5 m during the shock and an adjacent synclinal valley dropped down 1 m (*19*), events analogous to those resulting from the Coalinga earthquake. The Chelif River, which has cut through the ridge, was dammed by upwarp of the anticline and formed a transient lake within the syncline. An uplifted late Quaternary river terrace across the anticline suggests that the ridge was built from repeated sudden slip events related to a concealed fault (*17*). The coseismic fault slip inferred from the horizontal and vertical geodetic displacements was about twice the 2-m magnitude of the reverse slip observed at the surface, and coseismic elevation changes across the fault implied that most of the fault slip was concentrated below 2 km (*19*). Spectacular examples of secondary faulting were left by the earthquake: normal faults with up to 5 m of slip on anticlinal folds and bedding-plane faults with up to 1 m of slip on fold limbs formed on the upthrown fault block (*18*).

Anticlinal uplift occurred at the epicentral (west) end of the 1952 Kern County, California, earthquake (M_s = 7.3), whereas the reverse and left-lateral fault ruptured to the surface at the east end of the aftershock zone, where Cretaceous granite is exposed. The earthquake focus lies beneath Wheeler Ridge, a fold in a 3-km-thick sequence of Pliocene and Quaternary sediments that was upwarped 1.0 m during the earthquake. Models of the horizontal and vertical geodetic data (*20, 21*) preclude fault rupture through the upper 5 km of sediments at the epicenter. Geologic correlation suggests that the central section of the fault has slipped at a rate of about 5 mm per year during the past 2 million years (*20*). In contrast to the epicentral area, the maximum ground displacement observed at the east end of the fault equals the modeled subsurface fault slip, and abundant fault scarps have formed there, consistent with Fig. 1B.

The 1964 Niigata earthquake (M_s = 7.5) struck in Japan's most widespread and rapidly deforming fold belt (*22*) (Fig. 3). Bathymetric surveys showed that the seabed was upwarped 3 to 5 m by the reverse slip event, but the surface deposits were not cut by faults except in a few isolated places (*7*). Awashima Island (Fig. 3) was tilted and uplifted 1.5 m. The sedimentary beds of the island, late Miocene in age, dip 10° to 20° (*23*), about 1000 times the amount they were tilted during the earthquake. This relation can be explained by progressive uplift and tilt during large slip events on a concealed reverse fault, similar to the style of deformation that we infer at Coalinga.

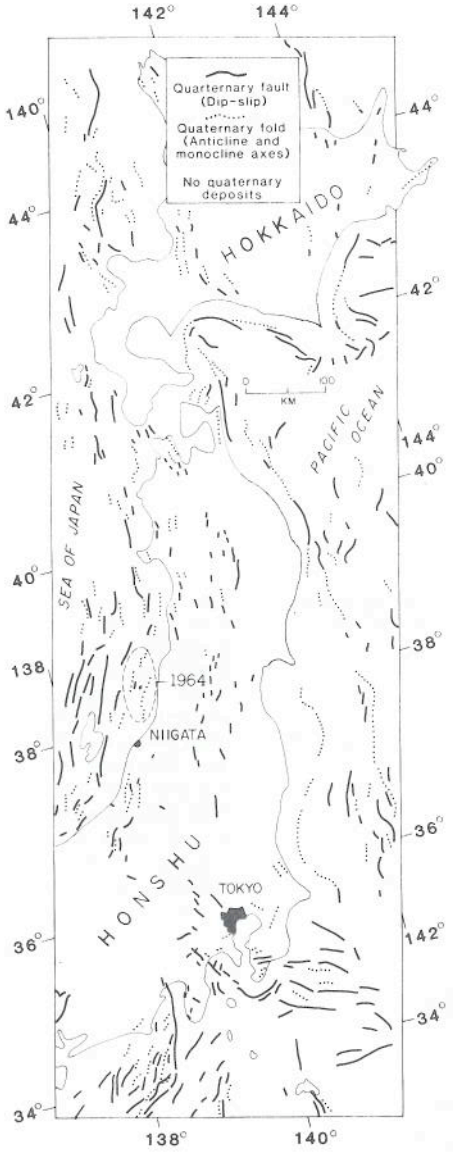

Fig. 3. Quaternary tectonic map of northern Japan (*25*) showing faults and folds in areas with Quaternary deposits. A dashed line encircles the aftershock zone of 1964 Niigata earthquake (M_s = 7.5) (*7*). Awashima Island is the dot within the zone.

The 1400-year-long historical record of earthquakes in Japan is equally well correlated with active faults and active folds (*24*); apparently folds provide as good an indicator of earthquake sources as do faults. The Quaternary tectonic map of northern Japan (*25*) also shows a similar number and distribution of dip-slip faults and folds (Fig. 3). These faults and fold axes are generally parallel to each other and orient normal to the azimuth of maximum compression inferred from horizontal geodetic measurements and shallow earthquakes. The shortest fold wavelengths (15 km) and highest historic and Quaternary uplift rates (1 to 3 mm per year) were measured in areas with the greatest accumulation of Neogene and younger (0 to 24 million years old) sediments (*22*).

Earthquakes on thrust faults leave an incomplete displacement record because slip at the seismic source generally diminishes or disappears at the ground surface. Folds form as a consequence of the diminished surface slip. Although the deformed surface materials can mask active faults, folds also provide evidence to assess the subsurface rate of fault slip. The record of damaging thrust earthquakes that did not rupture through surface deposits argues for intensified investigation of contemporary and Quaternary deformation within the world's active fold belts.

ROSS S. STEIN

U.S. Geological Survey, Menlo Park, California 94025

GEOFFREY C. P. KING

Bullard Laboratories, Department of Earth Science, Cambridge University, Cambridge, England CB3 OEZ

References and Notes

1. R. S. Stein, in *Calif. Div. Mines Geol. Spec. Publ. 66* (1983), pp. 151–164.
2. A 5 km-long fault ruptured at the surface during an aftershock on 10 June 1983, 15 km west of the 2 May 1983 main shock (Fig. 2A). This fault, which dips northeast and displays 0.6 m of reverse dip slip in Cretaceous sediments, does not appear to extend from the main fault plane [E. W. Hart and R. D. McJunkin, *ibid.*, pp. 201–219].
3. A. McGarr, *J. Geophys. Res.*, in press.
4. W. Thatcher, *ibid.* **80**, 4862 (1979).
5. Surface breakage for the well-documented 1971 San Fernando, Calif., earthquake (M_s = 6.5) represented only half the subsurface slip estimated from geodetic data [R. V. Sharp, *Calif. Div. Mines Geol. Bull.* **96**, 187 (1975); J. C.

Savage, R. O. Burford, W. T. Kinoshita, *ibid.*, p. 175].
6. R. S. Yeats, *J. Geophys. Res.* **88**, 569 (1983); *Science* **196**, 295 (1979).
7. K. Satake and K. Abe [*J. Phys. Earth* **31**, 217 (1983) examine the Niigata earthquake and its aftershocks.
8. A. Cisternas [*Bull. Seismol. Soc. Am.* **53**, 1075 (1963)] examined the Kern County earthquake. M. Ouyed, G. Yielding, D. Hatzfield, and G. C. P. King [*Geophys. J. R. Astron. Soc.* **73**, 605 (1983)] investigated El Asnam aftershocks.
9. J. Eaton, R. Cockerham, F. Lester, in *Calif. Div. Mines Geol. Spec. Publ. 66* (1983), pp. 261–274; R. A. Uhrhammer, R. B. Darragh, B. A. Bolt, *ibid.*, pp. 221–232.
10. S. H. Hartzell and T. H. Heaton, *ibid.*, pp. 241–246; H. Kanamori, *ibid.*, pp. 233–240.
11. E. Fielding, M. Barazangi, L. Brown, J. Oliver, and S. Kaufman (*ibid.*, pp. 137–150) and C. M. Wentworth, A. W. Walter, J. A. Bartow, and M. D. Zoback (*ibid.*, pp. 113–126) interpret seismic refraction and reflection profiles beneath the Kettleman Hills anticline, 65 km south of the Coalinga main shock, as showing a steeply northeast dipping reverse fault with 0.5 to 1.0 km of displacement and a gently southwest dipping thrust fault with about 10 km of cumulative slip.
12. G. King and R. Stein, *ibid.*, pp. 165–176.
13. A. W. Burnett and S. A. Schumm [*Science* **222**, 49 (1983)] use similar techniques in the central United States.
14. Time-stratigraphic correlation of the Holocene Panoche alluvial-fan surface (Fig. 2A) from the soil survey of the Coalinga area [*U.S. Dept. Agric. Ser. 1944* (1952) and the age of the Tulare Formation are reviewed by W. R. Lettis [*U.S. Geol. Surv. Open-File Rep. 82-526* (1982)]. B. Atwater (in preparation) furnished the radiocarbon age.
15. The earthquake elevation changes are closely correlated with topography. After a regional slope of 0.37° is removed from the leveling route topography, the topographic height is equal to about 300 times the 1983 elevation change. The amplitude of the topography is damped relative to the structural contours, however, by erosion from the ridge crest and deposition into lows. The late Pleistocene beds of the Tulare Formation dip 4 to 16 times more steeply than the topographic slope of the anticline. Thus, the minimum cumulative fault slip since deposition of the beds becomes 1.8 m × 300 × 4 = 2 km.
16. T. W. Dibblee, *U.S. Geol. Surv. Open-File Rep. 71–87* (1971).
17. G. C. P. King and C. Via-Finzi, *Nature (London)* **292**, 22 (1981); G. Yielding, J. A. Jackson, G. C. P. King, H. Sinvhal, C. Vita-Finzi, R. M. Wood, *Earth Planet. Sci. Lett.* **56**, 287 (1981); Y. Thommeret, G. C. P. King, C. Vita-Finzi, *ibid.* **63**, 137 (1983).
18. H. Philip and M. Meghraoui, *Tectonics* **2**, 17 (1983).
19. J. C. Ruegg, M. Kasser, A. Tarantola, J. C. Lepine, B. Chouikrat, *Bull. Seismol. Soc. Am.* **72**, 2227 (1982).
20. R. S. Stein and W. Thatcher, *J. Geophys. Res.* **86**, 4913 (1981).
21. W. S. Dunbar, D. M. Boore, W. Thatcher, *ibid.* **70**, 1893 (1980).
22. Y. Ota [*GeoJournal* **4**, 111 (1980)] reviewed the deformed Quaternary shorelines; T. Kato [*Tectonophysics* **97**, 183 (1983)] measured the historic shoreline deformation from tide gage records.
23. H. Kawasumi, Ed., *General Report on the Niigata Earthquake of 1964* (Tokyo Electrical Engineering College Press, Tokyo, 1973); *Submarine Geological Chart of the Adjacent Seas of Nippon* (Marine Safety Agency, Tokyo, 1973).
24. Compare the distribution of released seismic energy by historic earthquakes (figure 5-13), to the distribution of faults (figure 5-14) and folds (figure 5-15), in *Explanatory Text of the Quaternary Tectonic Map of Japan* (National Research Center for Disaster Prevention, Tokyo, 1973).
25. Research Group for Quaternary Tectonic Map, *Quaternary Tectonic Map of Japan* (National Research Center for Disaster Prevention, Tokyo, 1969); Research Group for Active Faults, *Active Faults in and Around Japan* (Univ. of Tokyo Press, Tokyo, 1980).
26. We are indebted to S. Lack, G. Mavko, A. McGarr, R. Wallace, C. Wentworth, R. Yerkes, and J. Ziony for incisive reviews. This is Cambridge Earth Sciences contribution 492. The order of authorship was chosen by lot. This work was supported by the Royal Society of London and National Environment Research Council grant GR3-3904.

13 January 1984; accepted 23 February 1984